ISSN 1063-7761, Journal of Experimental and Theoretical Physics, 2015, Vol. 121, No. 2, pp. 229–236. © Pleiades Publishing, Inc., 2015.
Original Russian Text © L.Yu. Barash, I.M. Khalatnikov, 2015, published in Zhurnal Eksperimental'noi i Teoreticheskoi Fiziki, 2015, Vol. 148, No. 2, pp. 266–274.

ORDER, DISORDER, AND PHASE TRANSITION IN CONDENSED SYSTEM

Effective Conductivity of the Rectangular and Hexagonal Tessellations in the Plane

L. Yu. Barash* and I. M. Khalatnikov

Landau Institute for Theoretical Physics, Chernogolovka, Moscow oblast, 142432 Russia
Science Center in Chernogolovka, Chernogolovka, Moscow oblast, 142232 Russia
**e-mail: barash@itp.ac.ru*

Received December 11, 2014

Abstract—The effective conductivity of the two-dimensional periodic polygonal tessellations in the plane is determined using the perturbation theory and numerically. A diagram technique in perturbation theory for the effective conductivity of the tesselations in the plane is established using oblique coordinates. Calculations for the three color hexagonal tesselation have been carried out. A numerical method is developed for obtaining effective conductivity with high accuracy both when the perturbation theory is applicable and when the conductivities of the tessellation components are substantially different. For small differences between the conductivities of the components, the approach of the perturbation theory agrees with the numerical results.

DOI: 10.1134/S1063776115080014

1. INTRODUCTION

The theory of the effective conductivity of heterogeneous systems and composites was studied in numerous works (see, e.g., [1–3]). The early theoretical works dealing with the theory of conductivity of macroscopic random media considered weakly inhomogeneous media and the simplest systems with a low concentration of spherical inclusions and proposed approximate analytical approaches to describing their properties [4–6]. Later, interest in such systems increased due to studying the metal–insulator phase transition that occurs when the inclusion concentration changes [7]. In the recent decade, prominence was given to the effective conductivity of composite materials with carbon nanotubes and graphene nanosheets and to the effective conductivity of colloidal nanoliquids due to the development of nanotechnologies [8–10].

The problem of the conductivity of two-dimensional (2D) composites has also received much attention. A number of exact analytical results, such as the duality relation, were obtained for the conductivity of 2D binary systems [11–16]. As follows from the duality relation, the effective conductivity of a random heterogeneous 2D medium with equal component concentrations (or of a periodic system with a chessboard structure) is the geometric mean of the component conductivities. 2D random systems and periodic lattices belong to the same class of universality near a phase-transition point [12, 17]. The effective conductivity of a number of 2D doubly periodic systems, which mainly contain dielectric or ideally conducting inclusions, was analytically found [3]. For a chessboard structure, the exact dependence of the effective conductivity on the ratio $h = \sigma_1/\sigma_2$ (where $\sigma_{1,2}$ are the conductivities of the composite components) is known, and the asymptotics of electric field near lattice corners, which leads to a breakdown of the linear current flow regime at low values of h, is also known [12, 14, 17–19].

In this work, we develop two approaches to studying the effective conductivity of 2D composites. The first approach uses the perturbation theory in parameter $1 - h$ and is based on the diagram technique (reviewed in Section 2) developed in [20]. In Section 3, we establish the rules to construct perturbation theory diagrams for the effective conductivity of plane tessellations using oblique coordinates. Using these rules, in Section 4 we calculate the three-color hexagonal tessellation of plane. Section 5 describes the second approach, namely, a numerical method for calculating the effective conductivity of 2D polygonal tesselations in the plane. For periodic structures, we use the finite difference method with relaxation to solve the Laplace equation with the corresponding matching conditions between components of the composite and with the corresponding periodic boundary conditions. This method makes it possible to obtain the effective conductivity with high accuracy both when the perturbation theory is applicable and when the component conductivities are significantly different. In Section 6, we test the developed approach for periodic plane tessellations with two and three colors and compare with analytical results.

For a locally isotropic medium, Ohm's law has the form

$$\mathbf{j} = -\sigma\nabla\varphi.$$

For a stationary distribution of currents, the continuity equation is

$$\mathrm{div}\mathbf{j} = 0.$$

Hence, we have

$$\Delta\varphi + \nabla\ln\sigma\cdot\nabla\varphi = 0.$$

We now write potential φ in the form

$$\varphi = -\mathscr{E}\cdot\mathbf{r} + \psi(x, y),$$

where the mean field is $\mathscr{E} = -\langle\nabla\varphi\rangle$, i.e., $\langle\nabla\psi\rangle = 0$. Here, the angle parentheses mean averaging over the entire plane. As a result, we obtain the following equation for $\psi(x, y)$:

$$\Delta\psi + \nabla\ln\sigma\cdot(-\mathscr{E} + \nabla\psi) = 0. \quad (1)$$

If a spatial conductivity distribution is isotropic on average, effective conductivity σ_{eff} is a scalar and determined by the relation $\mathbf{J} = \sigma_{\mathrm{eff}}\mathscr{E}$, where $\mathbf{J} = \langle\mathbf{j}\rangle$. If $\psi(x, y)$ is known, we can determine the effective conductivity from the relation

$$\sigma_{\mathrm{eff}}\mathscr{E} = \langle\mathbf{j}\rangle = \langle\sigma\rangle\mathscr{E} - \langle\sigma\nabla\psi\rangle. \quad (2)$$

2. PERTURBATION THEORY

Let us briefly review the perturbation theory developed for the effective conductivity in [20]. When considering the perturbation theory, we assume

$$\varphi = -\mathbf{E}\cdot\mathbf{r} + \psi_c(x, y),$$

where $\mathbf{E}$ is the mean electric field without regard for the influence of deviations from the average conductivity, i.e., at $\sigma(x, y) = \langle\sigma(x, y)\rangle$. We then assume

$$\langle\sigma(x, y)\rangle = 1, \quad \alpha(x, y) = \sigma(x, y) - 1.$$

Applying the Fourier transformations to the continuity equation for small quantities α and ψ_c, we obtain

$$k^2\psi_{c,\mathbf{k}} = \left[\nabla\left(\alpha - \frac{\alpha^2}{2} + \frac{\alpha^3}{3} - \frac{\alpha^4}{4} + \ldots\right)\cdot(-\mathbf{E} + \nabla\psi_c)\right]_{\mathbf{k}}. \quad (3)$$

Solving Eq. (3) by iterations in the powers of small parameter α, we find the expansion of the main quantities in the perturbation theory,

$$\sigma_{\mathrm{eff},c} = \sum_{n=0}^{\infty}\sigma_{\mathrm{eff},c}^{(n)}, \quad \psi_c = \sum_{n=1}^{\infty}\psi_c^{(n)}.$$

Here, we have

$$\nabla\psi_c^{(0)} = (i\mathbf{k}\psi_{c,\mathbf{k}}^{(0)})_{\mathbf{k}\to 0} = -\mathbf{E}, \quad \sigma_{\mathrm{eff},c}^{(0)} = 1,$$

and every next order of the perturbation theory is expressed through the previous order by the formulas

$$\psi_{c,\mathbf{k}}^{(n)} = -\sum_{\mathbf{p}}\frac{\mathbf{k}\cdot\mathbf{p}}{k^2}\alpha_{\mathbf{k}-\mathbf{p}}\psi_{c,\mathbf{p}}^{(n-1)}, \quad (4)$$

$$\sigma_{\mathrm{eff},c}^{(n)} = -i\sum_{\mathbf{k}}\frac{\mathbf{k}\cdot\mathbf{E}}{E^2}\psi_{c,\mathbf{k}}^{(n-1)}\alpha_{-\mathbf{k}}. \quad (5)$$

Therefore, we have

$$\sigma_{\mathrm{eff},c}^{(n)} = (-1)^{n+1} \times \sum_{\mathbf{k}_1,\ldots,\mathbf{k}_{n-1}}\frac{(\mathbf{k}_1\cdot\mathbf{E})(\mathbf{k}_1\cdot\mathbf{k}_2)\ldots(\mathbf{k}_{n-2}\cdot\mathbf{k}_{n-1})(\mathbf{k}_{n-1}\cdot\mathbf{E})}{E^2\mathbf{k}_1^2\ldots\mathbf{k}_{n-1}^2} \times \alpha_{\mathbf{k}_1}\alpha_{\mathbf{k}_2-\mathbf{k}_1}\ldots\alpha_{\mathbf{k}_{n-1}-\mathbf{k}_{n-2}}\alpha_{-\mathbf{k}_{n-1}}. \quad (6)$$

Equation (6) describes the contributions of all connected diagrams in each order of the perturbation theory. Generally speaking, the obtained quantity ψ_c does not meet the condition $\langle\nabla\psi_c\rangle = 0$. Hence, the mean electric field is

$$\mathscr{E} = \langle\nabla(\mathbf{E}\cdot\mathbf{r} - \psi_c(x, y))\rangle = \mathbf{E} - \langle\nabla\psi_c\rangle,$$

for the effective conductivity, we have

$$\sigma_{\mathrm{eff}}(\mathbf{E} - \langle\nabla\psi_c\rangle) = \mathbf{E} - \langle(1 + \alpha)\nabla\psi_c\rangle,$$

and the quantity found by Eq. (6) is

$$\sigma_{\mathrm{eff},c}\mathbf{E} = \mathbf{E} - \langle\alpha\nabla\psi_c\rangle.$$

Therefore, we have

$$\langle\nabla\psi_c\rangle = \frac{\sigma_{\mathrm{eff}} - \sigma_{\mathrm{eff},c}}{\sigma_{\mathrm{eff}} - 1}\mathbf{E} \quad (7)$$

and, in particular, vector $\langle\nabla\psi_c\rangle$ is directed along vector $\mathbf{E}$. Note now that, in the polar coordinates, we obtain

$$\langle\nabla\psi_c\rangle = \sum_{\mathbf{k}} i\mathbf{k}\psi_{c,\mathbf{k}}\delta(\mathbf{k}) = \frac{1}{\pi}\int_0^{2\pi}\int_0^{\infty} i\mathbf{k}\psi_{c,\mathbf{k}}\delta(k)dkd\varphi_{\mathbf{k}} = \frac{1}{2\pi}\int_0^{2\pi}(i\mathbf{k}\psi_{c,\mathbf{k}})_{\mathbf{k}\to 0}d\varphi_{\mathbf{k}}. \quad (8)$$

Therefore, using Eqs. (4) and (5) and the relationship

$$\int_0^{2\pi}\cos(t - t_1)\cos(t - t_2)dt = \pi\cos(t_1 - t_2),$$

we find

$$\langle\nabla\psi_c^{(n)}\rangle = -i\sum_{\mathbf{p}}\frac{\alpha_{-\mathbf{p}}\psi_{c,\mathbf{p}}^{(n-1)}}{2\pi}\int_0^{2\pi}(\mathbf{i}_{\mathbf{k}}\cdot\mathbf{p})\mathbf{i}_{\mathbf{k}}d\varphi_{\mathbf{k}} = -\frac{i}{2}\sum_{\mathbf{p}}\alpha_{-\mathbf{p}}\psi_{c,\mathbf{p}}^{(n-1)}\mathbf{p}, \quad (9)$$

$$\sigma_{\mathrm{eff},c}^{(n)}\mathbf{E} = 2(\langle\nabla\psi_c^{(n)}\rangle\cdot\mathbf{i}_{\mathbf{E}})\mathbf{i}_{\mathbf{E}} = 2\langle\nabla\psi_c^{(n)}\rangle, \quad (10)$$

where $\mathbf{i}_{\mathbf{k}}$ and $\mathbf{i}_{\mathbf{E}}$ are the unit vectors along $\mathbf{k}$ and $\mathbf{E}$. Hence, we have

$$\langle\nabla\psi_c\rangle = \frac{1}{2}(\sigma_{\mathrm{eff},c} - 1)\mathbf{E}.$$

When comparing the last expression with Eq. (7), we obtain

$$\sigma_{\mathrm{eff}} - \sigma_{\mathrm{eff},c} = \frac{1}{2}(\sigma_{\mathrm{eff}} - 1)(\sigma_{\mathrm{eff},c} - 1), \quad (11)$$

$$\sigma_{\text{eff}} = \frac{1+\sigma_{\text{eff},c}}{3-\sigma_{\text{eff},c}} = 1+\sum_{n=1}^{\infty}\frac{(\sigma_{\text{eff},c}-1)^n}{2^{n-1}}. \quad (12)$$

Equation (12) exactly corresponds to the following rule of the perturbation theory formulated in [20]: all disconnected diagrams consisting of two chains should be subtracted from the sum of n-order diagrams, the disconnected diagrams consisting of three chains should be then added, and so on. Note that the contribution of the diagrams consisting of n chains is the product of the contributions of these chains found by Eq. (6), multiplied by $(-1/2)^{n-1}$. The gaps between chains are assumed to correspond to zero-momentum propagators, each of which is 1/2. When these rules are applied, agreement with the Keller–Dykhne formula was obtained up to the tenth order in [20].

Let us dwell on Eq. (6) and introduce designations

$$T_i = \frac{1}{2}\frac{k_{ix}^2+k_{iy}^2}{k_i^2}, \quad G_i = \frac{k_{ix}k_{iy}}{k_i^2}, \quad F_i = \frac{1}{2}\frac{k_{ix}^2-k_{iy}^2}{k_i^2},$$

$$T_{ij} = k_{ix}k_{jx}+k_{iy}k_{jy}, \quad F_{ij} = k_{ix}k_{jx}-k_{iy}k_{jy},$$

$$G_{ij} = k_{ix}k_{jy}+k_{iy}k_{jx}, \quad H_{ij} = k_{ix}k_{jy}-k_{iy}k_{jx}.$$

The following identities hold true:

$$T_{i-1,i}T_{i,i+1}/k_i^2 = T_iT_{i-1,i+1}+G_iG_{i-1,i+1}+F_iF_{i-1,i+1}, \quad (13)$$

$$G_{i-1,i}T_{i,i+1}/k_i^2 = T_iG_{i-1,i+1}+G_iT_{i-1,i+1}-F_iH_{i-1,i+1}, \quad (14)$$

$$F_{i-1,i}T_{i,i+1}/k_i^2 = T_iF_{i-1,i+1}+G_iH_{i-1,i+1}+F_iT_{i-1,i+1}, \quad (15)$$

$$H_{i-1,i}T_{i,i+1}/k_i^2 = T_iH_{i-1,i+1}+G_iF_{i-1,i+1}-F_iG_{i-1,i+1}. \quad (16)$$

The application of these identities results in the rules of the replacement of propagators by the F-, G-, and T-propagators; the corresponding rules of sign; and the rules of an even number of F- and G-propagators that were formulated in [20].

For an anisotropic $\alpha(x, y)$ distribution, it is necessary to consider effective conductivity tensor $J_i = \sigma_{\text{eff},i,j}\mathscr{E}_j$. We can show that the right-hand side of Eq. (6) in this case determines the value of $E_i\sigma_{\text{eff},c,i,j}E_j/E^2$ and the expression

$$E_i(\sigma_{\text{eff},i,j}-\sigma_{\text{eff},c,i,j})E_j = \frac{1}{2}(\sigma_{\text{eff},i,j}-1)E_j(\sigma_{\text{eff},c,i,k}-1)E_k$$

is valid instead of Eq. (11). Therefore, the consideration of the perturbation theory for vector **E** directed along axis x makes it possible to determine $\sigma_{\text{eff},x,x}$, and the consideration for vector **E** directed along axis y, $\sigma_{\text{eff},y,y}$. To determine the effective conductivity tensor using the perturbation theory, it is convenient to sequentially find the quantities

$$\sigma_{\text{eff},I} = (\sigma_{\text{eff},x,x}+\sigma_{\text{eff},y,y})/2,$$

$$\sigma_{\text{eff},A} = (\sigma_{\text{eff},x,x}-\sigma_{\text{eff},y,y})/2, \quad \sigma_{\text{eff},x,y}.$$

3. PERTURBATION THEORY IN OBLIQUE COORDINATES

In some cases (e.g., for hexagonal tessellations), obtaining the effective conductivity using the perturbation theory in the Cartesian coordinates turns out to be an awkward and difficult procedure. The use of oblique coordinates and the correspondingly changed rules of the diagram technique significantly simplifies the solution of such problems. Let angle φ be the angle between the unit vectors of coordinate axes x and y. Then, the scalar product is written in the form

$$\mathbf{s}\cdot\mathbf{t} = s_xt_x+s_yt_y+(s_xt_y+s_yt_x)\cos\varphi,$$

in particular,

$$k_i^2 = k_{ix}^2+k_{iy}^2+2k_{ix}k_{iy}\cos\varphi.$$

We now introduce designations

$$\tilde{T}_i = T_i+G_i\cos\varphi = \frac{1}{2},$$

$$\tilde{G}_i = G_i+T_i\cos\varphi = \frac{k_{ix}k_{iy}\sin^2\varphi}{k_i^2}+\frac{\cos\varphi}{2},$$

$$\tilde{F}_i = F_i = \frac{1}{2}\frac{k_{ix}^2-k_{iy}^2}{k_i^2},$$

$$\tilde{T}_{ij} = T_{ij}+G_{ij}\cos\varphi, \quad \tilde{G}_{ij} = G_{ij}+T_{ij}\cos\varphi,$$

$$\tilde{F}_{ij} = F_{ij}\sin^2\varphi, \quad H_{ij} = H_{ij}\sin^2\varphi.$$

The following identities then hold true:

$$\tilde{T}_{i-1,i}\tilde{T}_{i,i+1}/k_i^2 = \tilde{T}_i\tilde{T}_{i-1,i+1}+\tilde{G}_i\tilde{G}_{i-1,i+1}+\tilde{F}_i\tilde{F}_{i-1,i+1}, \quad (17)$$

$$\tilde{G}_{i-1,i}\tilde{T}_{i,i+1}/k_i^2 = \tilde{T}_i\tilde{G}_{i-1,i+1}+\tilde{G}_i\tilde{T}_{i-1,i+1}-\tilde{F}_i\tilde{H}_{i-1,i+1}, \quad (18)$$

$$\tilde{F}_{i-1,i}\tilde{T}_{i,i+1}/k_i^2 = \tilde{T}_i\tilde{F}_{i-1,i+1}+\tilde{G}_i\tilde{H}_{i-1,i+1}+\tilde{F}_i\tilde{T}_{i-1,i+1}, \quad (19)$$

$$\tilde{H}_{i-1,i}\tilde{T}_{i,i+1}/k_i^2 = \tilde{T}_i\tilde{H}_{i-1,i+1}+\tilde{G}_i\tilde{F}_{i-1,i+1}-\tilde{F}_i\tilde{G}_{i-1,i+1}. \quad (20)$$

As a result, we can now use the usual rules of the diagram technique. Designating $\mathbf{k}_0 = \mathbf{k}_n = \mathbf{E}$, we obtain

$$\tilde{T}_{0,n} = E^2, \quad \tilde{G}_{0,n} = (E_x^2+E_y^2)\cos\varphi+2E_xE_y,$$

$$\tilde{F}_{0,n} = (E_x^2-E_y^2)\sin^2\varphi, \quad \tilde{H}_{0,n} = 0.$$

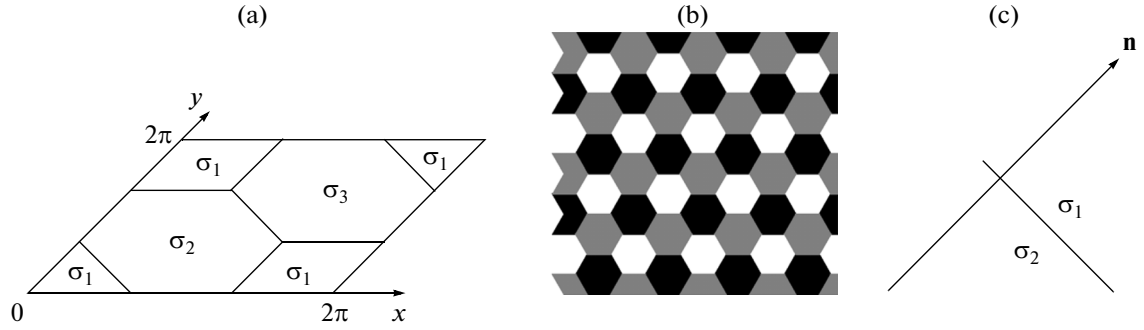

Fig. 1. (a, b) Three-color hexagonal tessellation. (c) Matching of ψ at the boundary between regions with conductivities σ_1 and σ_2.

Choosing vector **E** parallel to axis x, we have

$$E_x = E, \quad E_y = 0, \quad \tilde{T}_{0,n} = E^2,$$
$$\tilde{G}_{0,n} = E^2\cos\varphi, \quad \tilde{F}_{0,n} = E^2\sin^2\varphi.$$

Choosing vector **E** orthogonal to axis x, we have

$$E_x = -E\cot\varphi, \quad E_y = E/\sin\varphi,$$
$$\tilde{T}_{0,n} = E^2, \quad \tilde{G}_{0,n} = -E^2\cos\varphi, \quad \tilde{F}_{0,n} = -E^2\sin^2\varphi.$$

Thus, for the isotropic part of the effective conductivity tensor, we obtain

$$\tilde{T}_{0,n} = E^2, \quad \tilde{G}_{0,n} = \tilde{F}_{0,n} = \tilde{H}_{0,n} = 0.$$

In particular, in the second order of the perturbation theory, we find

$$\sigma^{(2)}_{\text{eff},I} = -\frac{1}{2}\sum_{\mathbf{k}}\alpha_{\mathbf{k}}\alpha_{-\mathbf{k}}. \tag{21}$$

4. THREE-COLOR HEXAGONAL TESSELLATION

Let $\alpha(x, y)$ be a periodic function with a period 2π, which is defined in domain $0 \le x < 2\pi$, $0 \le y < 2\pi$ as

$$\alpha(x, y) = \alpha_1,$$

if $x + y < 2\pi/3$ or $x + y > 10\pi/3$, or $x > 4\pi/3$, $y < 2\pi/3$, or $x < 2\pi/3$, $y > 4\pi/3$;

$$\alpha(x, y) = \alpha_3,$$

if $x + y > 2\pi$ and $\alpha(x, y) \neq \alpha_1$; and

$$\alpha(x, y) = \alpha_2,$$

if $\alpha(x, y) \neq \alpha_1$ and $\alpha(x, y) \neq \alpha_3$ (Fig. 1). We also assume that the condition

$$\langle\alpha(x, y)\rangle = (\alpha_1 + \alpha_2 + \alpha_3)/3 = 0$$

is met. Then, the unit cell is a rhomb with an angle $\varphi = \pi/3$, which is equal to the angle between coordinate axes x and y. The Fourier components in the oblique coordinates have the form

$$\alpha_{k_x, k_y} = \beta_{k_x + k_y\cos\varphi,\, k_y + k_x\cos\varphi},$$

where

$$\beta_{n,m} = \frac{1}{(2\pi)^2}\int\alpha(x, y)e^{-i(nx+my)}dxdy,$$

and numbers $n = k_x + k_y\cos\varphi$ and $m = k_y + k_x\cos\varphi$ are integers. Thus, the Fourier coefficients for the three-color hexagonal tessellation have the form

$$\beta_{3n,3m} = \beta_{3n+2,3m+1} = \beta_{3n+1,3m+2} = 0, \tag{22}$$

$$\beta_{3n+1,3m+1} = \frac{3[2\alpha_1 + (i\sqrt{3} - 1)\alpha_2 - (1 + i\sqrt{3})\alpha_3]}{8(3m + 1)(3n + 1)\pi^2} + \frac{[2\sqrt{3}\alpha_1 - (\sqrt{3} - 3i)\alpha_2 - (\sqrt{3} + 3i)\alpha_3]\delta_{n,m}}{12\pi(3n + 1)}, \tag{23}$$

$$\beta_{3n+2,3m+2} = \frac{3[2\alpha_1 - (i\sqrt{3} + 1)\alpha_2 + (i\sqrt{3} - 1)\alpha_3]}{8(3m + 2)(3n + 2)\pi^2} + \frac{[-2\sqrt{3}\alpha_1 + (\sqrt{3} + 3i)\alpha_2 + (\sqrt{3} - 3i)\alpha_3]\delta_{n,m}}{12\pi(3n + 2)}, \tag{24}$$

$$\beta_{3m,3n+1} = \beta_{3n+1,3m} = \beta^*_{3n+1,3(n-m)+1},$$
$$\beta_{3m,3n+2} = \beta_{3n+2,3m} = \beta^*_{3n+2,3(n-m)+2}. \tag{25}$$

Let $A = -3(\alpha_1\alpha_2 + \alpha_1\alpha_3 + \alpha_2\alpha_3)$. Then, in the second order of the perturbation theory, we have

$$\sum_{n,m=-\infty}^{\infty}\beta_{3n+1,3m}\beta_{-3n-1,-3m} = \sum_{n,m=-\infty}^{\infty}\beta_{3n+2,3m}\beta_{-3n-2,-3m} = \frac{A}{27}, \tag{26}$$

$$\sum_{n,m=-\infty}^{\infty}\beta_{3n,3m+1}\beta_{-3n,-3m-1} = \sum_{n,m=-\infty}^{\infty}\beta_{3n,3m+2}\beta_{-3n,-3m-2} = \frac{A}{27}, \tag{27}$$

$$\sum_{n,m=-\infty}^{\infty} \beta_{3n+1,3m+1}\beta_{-3n-1,-3m-1} = \sum_{n,m=-\infty}^{\infty} \beta_{3n+2,3m+2}\beta_{-3n-2,-3m-2} = \frac{A}{27}, \quad (28)$$

$$\sigma^{(2)}_{\text{eff},I} = -\frac{1}{2}\sum_{m,n=-\infty}^{\infty} \beta_{n,m}\beta_{-n,-m} = -\frac{A}{9} = -\frac{1}{6}(\alpha_1^2+\alpha_2^2+\alpha_3^2). \quad (29)$$

The last equation coincides with the general expression for the effective conductivity of a 2D isotropic weakly inhomogeneous medium [5, §9],

$$\sigma_{\text{eff},I} = \langle\sigma\rangle\left(1-\frac{1}{2}\frac{(\sigma-\langle\sigma\rangle)^2}{\langle\sigma\rangle^2}\right). \quad (30)$$

5. NUMERICAL DETERMINATION OF THE EFFECTIVE CONDUCTIVITY

For the problem with a periodic tessellation of plane, Eq. (1) is reduced to the Laplace equation $\Delta\psi = 0$ in each region of constant values of σ with corresponding matching conditions between such regions. For a numerical simulation, we use Cartesian coordinates x and y. The condition $\langle\nabla\psi\rangle = 0$ is met, since numerically found quantity $\psi(x, y)$ is a periodic function of both coordinates. To find the effective conductivity numerically, it is sufficient to find $\langle\nabla\psi\rangle$ in each region where σ is constant and to apply Eq. (2). We now derive a matching condition for the case of a straight-line boundary between the regions (see Fig. 1c). Without loss of generality, we have $n = 0$ at the boundary, near which $\sigma(n) = \sigma_2 + (\sigma_1 - \sigma_2)\theta(n)$, where $\theta(n)$ is the Heaviside function. Then, we have $\partial\sigma/\partial n = (\sigma_1 - \sigma_2)\delta(n)$ and, hence,

$$\int_{-\varepsilon}^{\varepsilon}\left[\Delta\psi + \frac{(\sigma_1-\sigma_2)\delta(n)}{\sigma(n)}\left(-\mathscr{E}_n + \frac{\partial\psi}{\partial n}\right)\right]dn = 0, \quad (31)$$

$$\frac{\partial\psi}{\partial n}\bigg|_{-\varepsilon}^{\varepsilon} + \frac{2(\sigma_1-\sigma_2)}{\sigma_1+\sigma_2} \times\left\{-\mathscr{E}_n + \frac{1}{2}\left[\left(\frac{\partial\psi}{\partial n}\right)_{+0} + \left(\frac{\partial\psi}{\partial n}\right)_{-0}\right]\right\} = 0, \quad (32)$$

$$\sigma_1\left(\frac{\partial\psi}{\partial n}\right)_{+0} - \sigma_2\left(\frac{\partial\psi}{\partial n}\right)_{-0} = (\sigma_1-\sigma_2)\mathscr{E}_n. \quad (33)$$

Thus, at the boundary between the regions shown in Fig. 1c, quantity $\psi(x, y)$ is continuous and $\partial\psi/\partial n$ has a jump determined by Eq. (33). To solve Eq. (1), we apply the finite difference method with relaxation with the corresponding matching conditions at the region boundaries, and with corresponding periodic boundary conditions. In each region, we have the equation

$$\frac{1}{\kappa}\frac{\partial\psi}{\partial t} = \frac{\partial^2\psi}{\partial x^2} + \frac{\partial^2\psi}{\partial y^2}, \quad (34)$$

where time-dependent quantity $\psi = \psi(x, y, t)$ tends toward desired function $\psi(x, y)$ and κ is a constant parameter. Finite difference representations for the second derivatives for a regular mesh have the form

$$\hat{\delta}_x^2\psi_{i,j} = \frac{1}{h_x^2}(\psi_{i-1,j} - 2\psi_{i,j} + \psi_{i+1,j}), \quad (35)$$

$$\hat{\delta}_y^2\psi_{i,j} = \frac{1}{h_y^2}(\psi_{i,j-1} - 2\psi_{i,j} + \psi_{i,j+1}), \quad (36)$$

where h_x and h_y are the mesh steps along x and y. It is known that alternating direction implicit method consists of the following two parts.

At the first stage, the derivative with respect to x is implicitly taken into account and the finite difference representation of Eq. (34) is written as

$$\frac{\psi_{i,j}^{n+1/2} - \psi_{i,j}^{n}}{\kappa h_t/2} = \hat{\delta}_x^2\psi_{i,j}^{n+1/2} + \hat{\delta}_y^2\psi_{i,j}^{n}. \quad (37)$$

This expression can be rewritten as

$$c_i'\psi_{i-1,j}^{n+1/2} + \left(d_i' - \frac{2}{\kappa h_t}\right)\psi_{i,j}^{n+1/2} + e_i'\psi_{i+1,j}^{n+1/2} = b_i', \quad (38)$$

where

$$c_i' = e_i' = \frac{1}{h_x^2}, \quad d_i' = -\frac{2}{h_x^2}, \quad c_j'' = e_j'' = -\frac{1}{h_y^2},$$

$$d_j'' = \frac{2}{h_y^2}, \quad b_i' = c_j''\psi_{i,j-1}^{n} + \left(d_j'' - \frac{2}{\kappa h_t}\right)\psi_{i,j}^{n} + e_j''\psi_{i,j+1}^{n}.$$

The right-hand side of Eq. (38) is known since the value of ψ at step n is known. At the boundaries between the composite components, coefficients c_i', d_i', e_i', and b_i' are separately calculated using matching condition (33) and the value of ψ at step n. For each j, we apply the tridiagonal matrix algorithm to solve the set of Eqs. (38) and find ψ at step $n + 1/2$.

At the second stage, the derivative with respect to y is implicitly taken and the finite difference representation of Eq. (34) is

$$\frac{\psi_{i,j}^{n+1} - \psi_{i,j}^{n+1/2}}{\kappa h_t/2} = \hat{\delta}_x^2\psi_{i,j}^{n+1/2} + \hat{\delta}_y^2\psi_{i,j}^{n+1}. \quad (39)$$

This expression can be rewritten as

$$c_j''\psi_{i,j-1}^{n+1} + \left(d_j'' + \frac{2}{\kappa h_t}\right)\psi_{i,j}^{n+1} + e_j''\psi_{i,j+1}^{n+1} = b_j'', \quad (40)$$

where

$$b_j'' = c_i'\psi_{i-1,j}^{n+1/2} + \left(d_i' + \frac{2}{\kappa h_t}\right)\psi_{i,j}^{n+1/2} + e_i'\psi_{i+1,j}^{n+1/2},$$

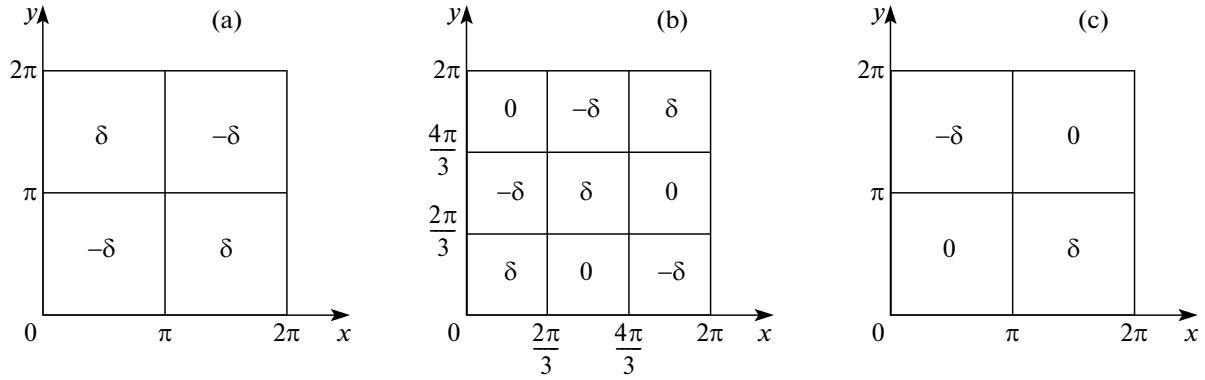

Fig. 2. Tessellations considered in [20]. $\alpha(x, y)$ distribution is shown; here, δ is a small coordinate-independent quantity.

is known since ψ at step $n + 1/2$ is known. At the composite component boundaries, coefficients c_j'', d_j'', e_j'', and b_j'', which enter linear Eq. (40), are separately calculated by applying matching condition (33). For each i, we apply the tridiagonal matrix algorithm to solve the set of Eqs. (40) and find ψ at step $n + 1$.

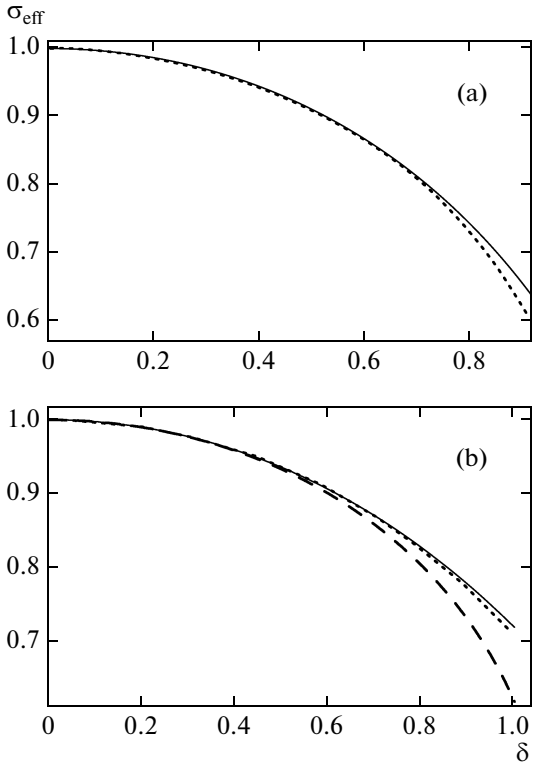

Fig. 3. Effective conductivity of the rectangular three-color tessellations shown in (a) Fig. 2b and (b) Fig. 2c as a function of parameter δ: (solid curves) perturbation theory calculations for small parameter δ, (dotted curves) numerical calculations, and (dashed curve) Bruggeman effective medium theory calculations.

For periodic boundary conditions, we have the matrix

$$\mathcal{A} = \begin{pmatrix} d_1 & e_1 & 0 & 0 & \ldots & c_1 \\ c_2 & d_2 & e_2 & 0 & \ldots & 0 \\ \ldots & \ldots & \ldots & \ldots & \ldots & \ldots \\ 0 & \ldots & 0 & c_{n-1} & d_{n-1} & e_{n-1} \\ e_n & \ldots & 0 & 0 & c_n & d_n \end{pmatrix} \quad (41)$$

instead of tridiagonal matrix $\mathcal{A}$ of the linear equation solved by the tridiagonal matrix algorithm. As was shown in [21], the solution of such a set of equations is reduced to the usual tridiagonal matrix algorithm applied to the truncated matrix

$$\mathcal{A}^c = \begin{pmatrix} d_1 & e_1 & 0 & 0 & \ldots & 0 \\ c_2 & d_2 & e_2 & 0 & \ldots & 0 \\ \ldots & \ldots & \ldots & \ldots & \ldots & \ldots \\ 0 & \ldots & 0 & c_{n-2} & d_{n-2} & e_{n-2} \\ 0 & \ldots & 0 & 0 & c_{n-1} & d_{n-1} \end{pmatrix}. \quad (42)$$

6. CALCULATION RESULTS

Figure 2 shows the tessellations considered in [20]. For a 2D two-color chessboard (Fig. 2a), the result of a numerical simulation of the effective conductivity coincides with that calculated by the Keller–Dykhne formula with high accuracy. This fact was repeatedly tested for many σ_1, σ_2 pairs. Figure 3 shows the effective conductivity calculated for a 2D three-color chessboard (Figs. 2b, 2c). The solid curve illustrates the effective conductivity calculated in [20] in the sixth (Fig. 3a) and fourth (Fig. 3b) orders of the perturbation theory. The dotted curve corresponds to the numerically calculated effective conductivity. The dashed curve in Fig. 3b depicts the effective conductivity calculated with the Bruggeman effective medium theory, which implies spherical inclusions. It

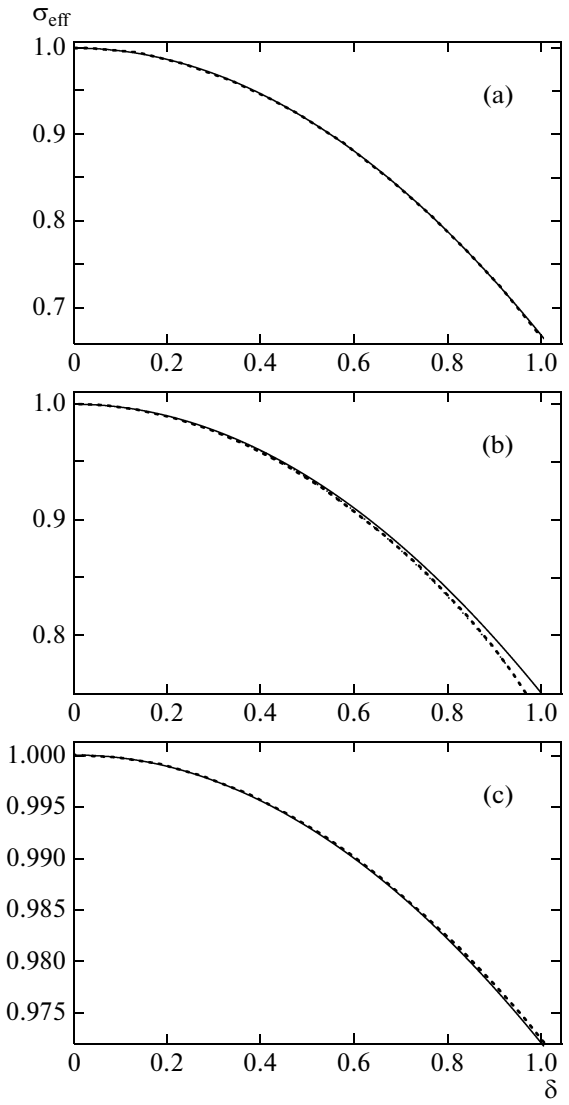

Fig. 4. Effective conductivity of the hexagonal tessellation shown in Fig. 1 as a function of parameter δ: (a) $\sigma_1 = 1 + \delta$, $\sigma_2 = 1 - \delta$, and $\sigma_3 = 1$; (b) $\sigma_1 = 1 + \delta/2$, $\sigma_2 = 1 - \delta$, and $\sigma_3 = 1 + \delta/2$; and (c) $\sigma_1 = 1 + \delta/3$, $\sigma_2 = 1 - 2\delta/15$, and $\sigma_3 = 1 - \delta/5$. Solid curves are calculated in perturbation theory for small parameter δ; dotted curves are calculated numerically.

is seen from these curves that the fourth order of the perturbation theory in this case more accurately describes the effective conductivity than the Bruggeman formula does (also see the discussion in [20]). At small differences between the conductivities of the composite components, the results of a numerical determination of the effective conductivity coincide with the results from [20].

Figure 4 shows the isotropic part of the effective conductivity of the hexagonal tessellation shown in Fig. 1 versus parameter δ. The solid line illustrates the effective conductivity calculated by Eq. (29), and the dotted curve was numerically calculated. Note the

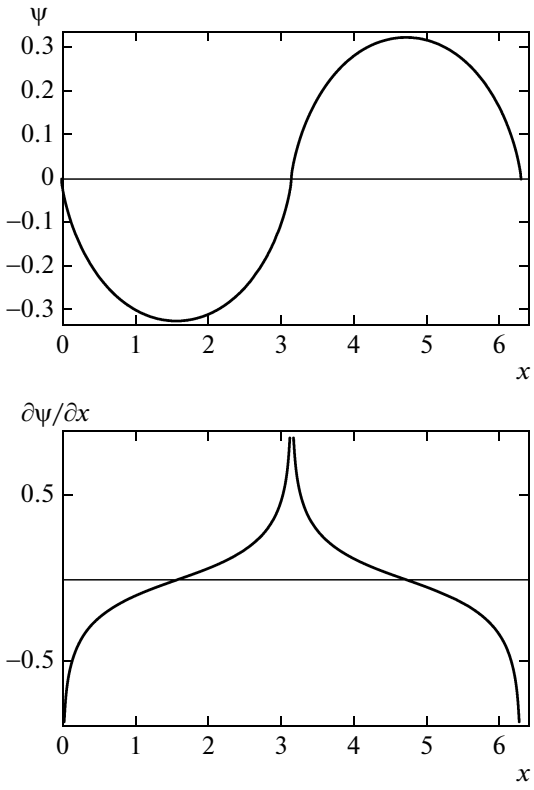

Fig. 5. ψ and $\partial\psi/\partial x$ calculated along a horizontal boundary for a chessboard structure with $\sigma_1 = 1.3$, $\sigma_2 = 0.7$, and a period 2π.

good agreement between the second order of the perturbation theory and the more accurate numerical calculation even in the region $\delta \approx 1$; generally speaking, this agreement could be unachieved.

Computer simulation supports the integrable divergence in the local electric field near the corners of composite component regions with a power relation that was obtained in [18]. Figure 5 shows quantities ψ and $\partial\psi/\partial x$ along a horizontal boundary, which illustrate the divergence of the local electric field near the corners of the boundaries in a two-color chessboard structure with $\sigma_1 = 1.3$, $\sigma_2 = 0.7$, and a period 2π. The divergences do not influence the development of a perturbation theory for the effective conductivity in the small parameter $(\sigma_2 - \sigma_1)/\sigma_2 = 1 - h$, since they are integrable and the exponent $(2/\pi)\arctan[(1-h)/2\sqrt{h}\,]$ in this case is small. Since the local-field singularities are integrable, a divergence does not appear in quantity ψ to be determined numerically.

The calculations demonstrate that the developed method allows us to describe with high accuracy the properties of periodic chessboard tessellations in the plane with two or three colors and of the hexagonal tessellation.

ACKNOWLEDGMENTS

The results presented in Sections 2, 5, and 6 were supported by the Russian Science Foundation, project no. 14-21-00158.

The simulations were performed using facilities of the Supercomputing Center of the Moscow State University [22].

REFERENCES

1. S. Torquato, *Random Heterogeneous Materials: Microstructure and Macroscopic Properties* (Springer-Verlag, Berlin, 2002).
2. D. S. Lia, G. Sahelia, M. Khaleelb, and H. Garmestani, Comput. Mater. Sci. **38**, 45 (2006).
3. Yu. P. Emets, *Electrical Characteristics of Composite Materials with a Regular Structure* (Naukova Dumka, Kiev, 1986) [in Russian].
4. Lord Rayleigh, Philos. Mag., Ser. 5 **34**, 481 (1892).
5. L. D. Landau and E. M. Lifshitz, *Course of Theoretical Physics*, Volume 8: *Electrodynamics of Continuous Media* (Butterworth–Heinemann, Oxford, 1984; Fizmatlit, Moscow, 2005).
6. S. Kirkpatrick, Rev. Mod. Phys. **45**, 574 (1973).
7. A. L. Efros and B. I. Shklovskii, Phys. Status Solidi B **76**, 475 (1976).
8. S. H. Xie, Y. Y. Liu, and J. Y. Li, Appl. Phys. Lett. **92**, 243121 (2008).
9. A. Bagchi and S. Nomura, Compos. Sci. Technol. **66**, 1703 (2006).
10. R. Prasher, W. Evans, P. Meakin, J. Fish, P. Phelan, and P. Keblinski, Appl. Phys. Lett. **89**, 143119 (2006).
11. J. B. Keller, J. Math. Phys. **5**, 548 (1964).
12. A. M. Dykhne, Sov. Phys. JETP **32**, 63 (1970).
13. V. G. Marikhin, JETP Lett. **71** (6), 271 (2000).
14. Yu. N. Ovchinnikov and A. M. Dyugaev, J. Exp. Theor. Phys. **90** (6), 1058 (2000).
15. Yu. N. Ovchinnikov and I. A. Luk'yanchuk, J. Exp. Theor. Phys. **94** (1), 203 (2002).
16. Yu. N. Ovchinnikov, J. Exp. Theor. Phys. **98** (1), 162 (2004).
17. Yu. P. Emets, Sov. Phys. JETP **69** (2), 397 (1989).
18. A. M. Satanin, V. V. Skuzovatkin, and S. V. Khor'kov, JETP Lett. **64** (7), 538 (1996).
19. A. M. Satanin, V. V. Skuzovatkin, and S. V. Khor'kov, J. Exp. Theor. Phys. **85** (2), 351 (1997).
20. I. M. Khalatnikov and A. Yu. Kamenshchik, J. Exp. Theor. Phys. **91** (6), 1261 (2000).
21. G. E. Karniadakis and R. M. Kirby II, *Parallel Scientific Computing in C++ and MPI* (Cambridge University Press, Cambridge, 2003).
22. V. Voevodin, S. Zhumatii, S. Sobolev, A. Antonov, P. Bryzgalov, D. Nikitenko, K. Stefanov, and V. Voevodin, Otkrytye Sist. **7**, 36 (2012).

Translated by K. Shakhlevich